Semarak Journal of Thermal-Fluid Engineering

Journal homepage: https://semarakilmu.my/index.php/sjotfe/index
ISSN: 3030-6639

# Modelling of Phase Change Material (PCM) Melting in an Internal Cavity

Wong Ling Mei[1], Ishkrizat Taib[1,*]

[1] Department of Mechanical Engineering, Faculty of Engineering Mechanical and Manufacturing, Universiti Tun Hussein Onn Malaysia, 86400 Parit Raja, Johor, Malaysia

**ARTICLE INFO**

***Article history:***
Received 26 April 2026
Received in revised form 5 May 2026
Accepted 22 May 2026
Available online 30 June 2026

***Keywords:***
Phase Change Material (PCM); Computational Fluid Dynamics (CFD); liquid-fraction evolution; thermal energy storage; solidification and melting

**ABSTRACT**

Latent Heat Thermal Energy Storage (LHTES) systems using phase change materials (PCMs) offer high energy storage density and stable operating temperatures, making them suitable for thermal energy management applications. This study investigates the melting behaviour of RT-50 PCM in a double-pipe LHTES system and evaluates the effect of heat transfer fluid (HTF) inlet velocity on the charging performance. A three-dimensional Computational Fluid Dynamics (CFD) model was developed in ANSYS Fluent using the laminar flow, energy, and solidification–melting models based on the enthalpy-porosity approach. A grid independence test was conducted using three mesh configurations, and a tetrahedral mesh containing 957,302 elements was selected for the final simulations. The melting process was analysed using liquid fraction contours and liquid fraction evolution curves for HTF inlet velocities of 20 m/s, 40 m/s, and 80 m/s. The results showed that the liquid fraction increased continuously from 0 to approximately 1.0, indicating complete melting of the PCM during the charging process. Comparison of the velocity cases revealed only minor differences in liquid fraction evolution despite a fourfold increase in HTF velocity from 20 m/s to 80 m/s. All cases exhibited similar melting trends and achieved complete melting within a comparable time period. The study concludes that PCM melting behaviour is influenced primarily by heat transfer within the PCM domain, while increasing HTF velocity provides only limited improvement in charging performance. The developed CFD model successfully captured the transient melting process and produced stable, grid-independent results.

## 1. Introduction

The increasing demand for energy and the growing emphasis on sustainable energy utilisation have led to significant interest in thermal energy storage (TES) technologies. Thermal energy storage systems improve energy efficiency by storing excess thermal energy during periods of low demand and releasing it when required. Among the various thermal energy storage techniques, latent heat thermal energy storage (LHTES) has attracted considerable attention due to its high energy storage density and ability to store large quantities of thermal energy within a narrow temperature range [1-3]. The performance of LHTES systems is primarily governed by the thermal characteristics of phase

* *Corresponding author.*
*E-mail address: iszat@uthm.edu.my*

https://doi.org/10.37934/sjotfe.9.1.2335a

change materials (PCMs), which absorb and release latent heat during melting and solidification processes.

Paraffin-based PCMs are among the most widely used thermal storage materials because of their high latent heat capacity, chemical stability, non-corrosive nature, and reliable thermal cycling performance [4,5]. However, the inherently low thermal conductivity of paraffin wax significantly limits the rate of heat transfer during charging and discharging processes, resulting in prolonged melting and solidification times [3,6]. Consequently, numerous studies have been conducted to investigate heat transfer enhancement techniques and improve the thermal performance of PCM-based storage systems. Recent review studies have further highlighted the importance of thermal conductivity enhancement methods, including fins, metal foams, nanoparticles, and geometric modifications, to improve the charging and discharging rates of latent heat storage systems [7-9].

Previous researchers have examined various latent heat thermal energy storage configurations using both experimental and numerical approaches. Trp [10] investigated the thermal response of shell-and-tube PCM storage systems and reported that natural convection strongly influences the melting process. Hosseini *et al.,* [11] demonstrated that the geometric arrangement of the storage unit significantly affects temperature distribution and melting rate. Similarly, Tay *et al.,* [12] found that heat transfer enhancement techniques can substantially reduce charging time and improve overall thermal storage performance. Mahdi *et al.,* [13] further reported that the incorporation of enhanced heat transfer surfaces can accelerate PCM melting by promoting more uniform heat distribution within the storage domain. Other studies have also shown that the thermal behaviour of PCM systems is strongly dependent on the interaction between conduction and buoyancy-driven convection within the molten PCM region [14].

Due to the complexity of coupled heat transfer, fluid flow, and phase change phenomena, Computational Fluid Dynamics (CFD) has become a widely adopted tool for investigating PCM thermal behaviour. CFD enables detailed analysis of temperature fields, velocity distributions, and phase interface evolution while reducing the time and cost associated with experimental investigations [15]. The development of the enthalpy-porosity method by Voller and Chander [16] significantly improved the ability of numerical models to simulate melting and solidification processes by eliminating the need to explicitly track the moving solid–liquid interface. Consequently, this approach has become one of the most commonly used numerical techniques in PCM simulations and has been extensively implemented in commercial CFD software such as ANSYS Fluent.

Several numerical studies have successfully applied the enthalpy-porosity formulation to investigate latent heat thermal energy storage systems. Arasu and Arun [17] demonstrated that CFD predictions showed good agreement with experimental measurements of PCM melting. Al-Abidi *et al.,* [18] reported that numerical simulations accurately captured the influence of natural convection on melting behaviour in shell-and-tube storage systems. Mahdi *et al.,* [13] employed ANSYS Fluent to analyse PCM melting in a double-pipe thermal energy storage system and found that heat transfer enhancement techniques significantly improved melting performance and reduced charging time. Their results further highlighted the importance of buoyancy-driven flow in accelerating the melting process and confirmed the suitability of the enthalpy-porosity model for PCM simulations. Similar conclusions have been reported by recent investigations focusing on PCM-based thermal energy storage systems under various operating conditions [19,20].

Despite the substantial amount of research conducted on PCM-based latent heat thermal energy storage systems, limited studies have specifically examined the influence of heat transfer fluid (HTF) velocity on the liquid fraction evolution of RT-50 paraffin wax in a double-pipe thermal energy storage configuration using a validated CFD framework. Furthermore, the relationship between HTF velocity and the overall melting progression remains insufficiently understood, particularly when the PCM thermal resistance dominates the charging process. Understanding this behaviour is important because increasing HTF velocity generally requires greater pumping power and operating costs, and therefore its actual influence on PCM melting performance must be properly evaluated.

The significance of this study lies in its ability to provide a clearer understanding of the melting characteristics of RT-50 paraffin wax under different HTF operating velocities using Computational Fluid Dynamics. The findings of this study can contribute to the optimisation of latent heat thermal energy storage systems by identifying whether increasing HTF velocity provides meaningful improvements in charging performance. Such information is valuable for the design and operation of energy storage systems where thermal efficiency and energy consumption must be balanced.

Therefore, the present study performs a CFD analysis of PCM melting in a double-pipe latent heat thermal energy storage system using ANSYS Fluent. The geometry and thermo-physical properties are adopted from the validated work of Trp [10], while the laminar flow, energy, and solidification–melting models are employed to predict the transient melting behaviour of RT-50 paraffin wax. The objectives of this study are to investigate the evolution of liquid fraction during the PCM melting process and to evaluate the influence of different HTF inlet velocities on the melting behaviour and charging performance of the thermal energy storage system.

## 2. Methodology

### *2.1 Governing Equations*

#### *2.1.1 Laminar flow model*

The flow behaviour of the heat transfer fluid (HTF) within the inner copper tube governs the rate at which thermal energy is supplied to the phase change material (PCM) during the charging process. The motion of the HTF is governed by the continuity equation, which expresses the principle of mass conservation. For an incompressible fluid, the continuity equation is shown in Eq. (1).

$$\frac{\partial \rho}{\partial t} + \nabla \cdot (\rho V) = 0 \tag{1}$$

where $V$ represents the velocity vector. This equation ensures that mass is conserved throughout the computational domain and that no artificial accumulation or depletion of fluid occurs during the numerical solution process. The conservation of momentum is described by the Navier–Stokes equations as shown in Eq. (2).

$$\rho\left(\frac{\partial V}{\partial t} + V \cdot \nabla V\right) = -\nabla p + \mu \nabla^2 V + \rho g \tag{2}$$

where $\rho$ is the fluid density, $p$ is pressure, $\mu$ is the dynamic viscosity, and $g$ is the gravitational acceleration vector. The equation represents the balance between inertial forces, pressure gradients, viscous forces, and body forces acting on the fluid.

#### *2.1.2 Energy equation*

Heat transfer within the latent heat thermal energy storage system occurs through a combination of convection, conduction, and latent heat absorption. The thermal energy carried by the HTF is transferred through the copper tube wall and subsequently absorbed by the PCM, resulting in temperature rise and phase transition. To describe this process, ANSYS Fluent solves the conservation of energy equation throughout both fluid and solid regions of the computational domain.

The energy equation is expressed in terms of total energy transport and includes contributions from thermal conduction, convective transport, viscous work, species diffusion, and volumetric heat sources. The general form of the energy equation can be written as Eq. (3).

$$\frac{\partial(\rho E)}{\partial t} + \nabla \cdot [V(\rho E + p)] = \nabla \cdot \left(k_{eff} \nabla T\right) + S_h \tag{3}$$

where $E$ denotes the total energy per unit mass, $k_{eff}$ is the effective thermal conductivity, $T$ is temperature, and $S_h$ represents volumetric heat source terms.

### *2.1.3 Solidification and melting model*

The phase transition process occurring within the PCM domain is simulated using the Solidification and Melting model available in ANSYS Fluent. This model is particularly suitable for latent heat thermal energy storage applications because it can accurately represent the absorption and release of latent heat during phase transition without explicitly tracking the moving solid–liquid interface. For a pure material or PCM with a narrow melting range, the liquid fraction is defined as Eq. (4).

$$\lambda = \begin{cases} 0, & T < T_{solid} \\ \frac{T - T_{solid}}{T_{liquid} - T_{solid}}, & T_{solid} < T < T_{liquid} \\ 1, & T > T_{liquid} \end{cases} \tag{4}$$

where $\lambda$ denotes the liquid fraction, while $T_{solid}$ and $T_{liquid}$ represent the solidus and liquidus temperatures, respectively.

### *2.1.4 Enthalpy-porosity method*

The enthalpy–porosity technique constitutes the mathematical foundation of the Solidification and Melting model implemented in ANSYS Fluent. According to the Fluent Theory Guide, this approach eliminates the need for explicit interface tracking by solving a single set of conservation equations throughout the entire computational domain while accounting for latent heat effects through the enthalpy formulation. The total enthalpy of the PCM is defined as the sum of sensible and latent heat contributions as shown in Eq. (5).

$$H = h + \Delta H \tag{5}$$

where $H$ is the total enthalpy, $h$ is the sensible enthalpy, and $\Delta H$represents latent heat content. The sensible enthalpy component is calculated as Eq. (6).

$$h = h_{ref} + \int_{T_{ref}}^{T} C_p \, dT \tag{6}$$

where $C_p$ is the specific heat capacity, $h_{ref}$ is the reference enthalpy, and $T_{ref}$ is the reference temperature. The latent heat contribution is expressed as Eq. (7).

$$\Delta H = \lambda L \tag{7}$$

where $L$ is the latent heat of fusion and λ is the liquid fraction.

*2.1.5 Momentum sink formulation in the mushy zone*

A unique feature of the enthalpy–porosity approach is the treatment of the mushy zone as a porous medium. During phase transition, the coexistence of solid and liquid phases restricts fluid motion within the PCM. To account for this phenomenon, ANSYS Fluent introduces an additional momentum sink term into the momentum equations. The momentum sink source term is expressed as Eq. (8).

$$S = A_{mushy} \frac{(1-\lambda)^2}{\lambda^3+\epsilon} V \qquad (8)$$

where $A_{mushy}$ is the mushy zone constant, $\lambda$ is the liquid fraction, and $\epsilon$ is a small numerical stabilisation parameter.

*2.2 Numerical Setup*
*2.2.1 Geometry*

The computational geometry was developed based on the latent heat thermal energy storage (LHTES) system investigated by Trp [10]. The model consists of a concentric double-pipe configuration comprising an inner copper tube for heat transfer fluid (HTF) flow and an outer cylindrical shell containing the phase change material (PCM). The geometry was constructed as a three-dimensional model with an axial length of 1 m to represent the thermal energy storage unit during the charging process.

Figure 1 illustrates the cross-sectional dimensions of the developed geometry. The inner tube has an inner diameter of 10 mm and an outer diameter of 12.5 mm, while the outer shell has an inner diameter of 50 mm and an outer diameter of 52.5 mm. The annular region between the inner tube and outer shell is occupied by RT-50 paraffin wax PCM. During operation, thermal energy is transferred from the hot HTF flowing through the inner tube to the surrounding PCM through the copper tube wall, resulting in PCM melting and thermal energy storage.

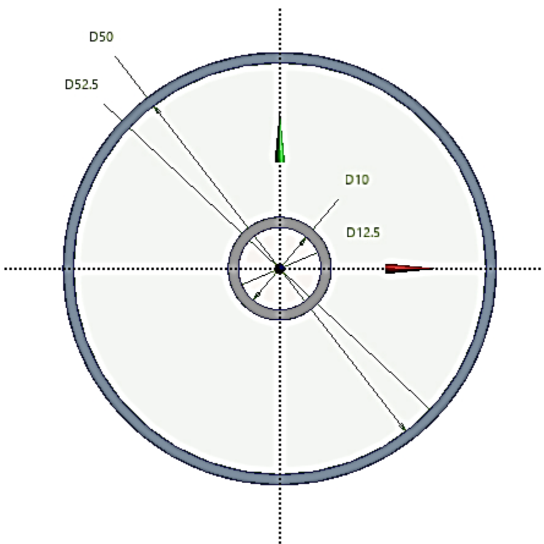


**Fig. 1.** Cross-sectional geometry

### *2.2.2 Mesh*

The computational domain was discretised using ANSYS Meshing to convert the physical geometry into a finite number of control volumes suitable for numerical analysis. Since mesh quality directly affects numerical accuracy and convergence behaviour, three different meshing approaches were investigated to evaluate their suitability for the PCM melting simulation. The first mesh configuration was generated using the default ANSYS meshing method with curvature-based sizing. This approach automatically refines the mesh in regions containing curved boundaries to improve geometric representation and numerical accuracy. Figure 2 presents the mesh generated using the default meshing strategy.

The second mesh configuration employed the Prime Mesh technology within the PCM region. Prime Mesh is designed to improve element quality and generate a more uniform mesh distribution while maintaining computational efficiency. The resulting mesh structure is shown in Figure 3. The third mesh configuration utilised tetrahedral elements within the PCM region. Tetrahedral meshes provide greater flexibility in resolving complex thermal gradients and phase interfaces, particularly in transient heat transfer simulations involving phase change phenomena. The generated tetrahedral mesh is illustrated in Figure 4.

The three mesh configurations were subsequently evaluated through a grid independence study to determine their influence on the predicted liquid fraction evolution during PCM melting. Based on the convergence behaviour and numerical stability obtained from the grid independence analysis, the tetrahedral mesh was selected as the final mesh topology for all subsequent simulations.

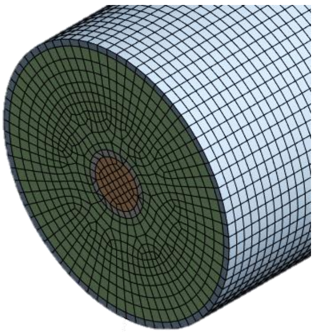

**Fig. 2.** Default mesh

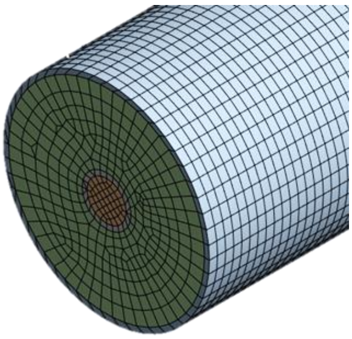

**Fig. 3.** Prime mesh

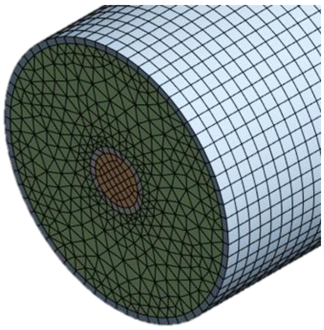

**Fig. 4.** Tetrahedrons

### *2.2.3 Boundary conditions*

The thermal and flow boundary conditions were established to simulate the charging process of the latent heat thermal energy storage (LHTES) system. The selected boundary conditions represent the operating conditions under which thermal energy is transferred from the heat transfer fluid (HTF) flowing inside the copper tube to the surrounding phase change material (PCM). Table 1 summarises the boundary conditions applied in the present CFD model.

Figure 5 illustrates the overall simulation setup and flow direction within the storage system. The hot heat transfer fluid enters the inner tube through the velocity inlet located at one end of the pipe and exits through the pressure outlet at the opposite end. During the charging process, thermal energy is continuously transferred from the HTF to the PCM through the copper tube wall, resulting in a gradual increase in PCM temperature and subsequent melting. The imposed flow direction ensures continuous transport of thermal energy throughout the length of the storage unit and enables the transient melting behaviour of the PCM to be investigated.

**Table 1**
Summary of boundary conditions applied

| Boundary region | Boundary type | Specification |
|---|---|---|
| HTF inlet | Velocity inlet | V = 20 m/s |
| | thermal condition | T = 450 K |
| HTF outlet | Pressure outlet | Gauge pressure = 0 Pa |
| Inner tube wall | Coupled wall | Heat transfer through conduction |
| | Adiabatic wall | Zero heat flux |
| PCM domain | Initial condition | Solid |
| | Initial temperature | T = 310 K |
| Gravity | Body force | Enable in -ve y direction |
| PCM model | Solidification and melting | Enthalpy-porosity method |

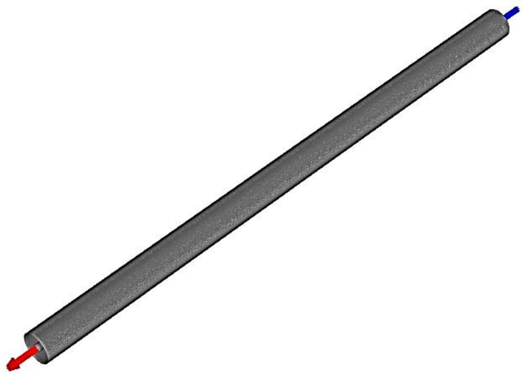

**Fig. 5.** Setup for simulations

*2.3 Grid Independence Test (GIT)*

A grid independence test was conducted to evaluate the influence of mesh density and mesh topology on the numerical prediction of the PCM melting process. The primary objective of this assessment was to ensure that the simulation results were independent of the computational grid and that the selected mesh provided sufficient numerical accuracy without incurring high computational cost. Three different mesh configurations were generated using different meshing strategies within ANSYS Meshing. The first configuration employed the default curvature-based meshing approach, while the second configuration utilised the Prime Mesh technology within the PCM region. The third configuration was generated using tetrahedral elements in the PCM domain. The characteristics of the investigated meshes are summarised in Table 2.

**Table 2**
Summary of mesh configuration used in GIT

| No. mesh | Meshing method | No. of nodes | No. of elements |
|---|---|---|---|
| Mesh 1 | Default ANSYS meshing | 437,451 | 419,814 |
| Mesh 2 | Prime mesh | 222,202 | 211,640 |
| Mesh 3 | Tetrahedrons | 237,565 | 957,302 |

To assess mesh sensitivity, the volume-averaged liquid fraction was selected as the monitoring parameter because it directly represents the progression of PCM melting throughout the charging process. The liquid fraction was monitored over the entire simulation period for each mesh configuration and subsequently compared. Since the liquid fraction is the principal indicator of thermal energy storage performance, its evolution provides an effective measure of numerical consistency between different computational grids.

Figure 6 illustrates the variation of volume-averaged liquid fraction as a function of melting time for the three mesh configurations. The results indicate that all meshes predict a similar overall melting trend, characterised by a gradual increase in liquid fraction followed by complete melting of the PCM. However, noticeable differences are observed during the intermediate stages of the melting process, particularly between approximately 500 s and 1500 s. These deviations demonstrate the influence of mesh resolution and element topology on the numerical prediction of the phase change process.

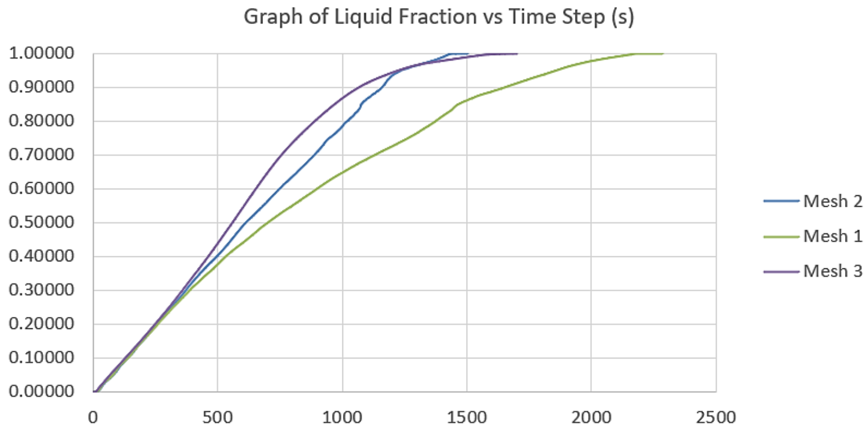


**Fig. 6.** Grid Independence Test (GIT)

The default curvature-based mesh and Prime Mesh configuration exhibit greater variation in the predicted liquid fraction profiles throughout the transient simulation. Although both meshes successfully capture the overall melting behaviour, local fluctuations in the liquid fraction evolution indicate a higher sensitivity to discretisation errors. In contrast, the tetrahedral mesh demonstrates a smoother and more physically consistent melting profile. The liquid fraction evolution predicted by the tetrahedral mesh shows a gradual and stable transition from the solid state to complete melting without significant oscillatory behaviour. This improved convergence behaviour suggests that the tetrahedral mesh provides enhanced spatial resolution of the temperature gradients and phase interface evolution within the PCM domain.

The superior performance of the tetrahedral mesh can be attributed to its ability to conform more effectively to the complex thermal gradients that develop during the melting process. As natural convection becomes dominant within the liquid PCM region, accurate representation of temperature and velocity fields becomes increasingly important. The tetrahedral mesh provides greater geometric flexibility and improved resolution of the solid–liquid interface, thereby reducing numerical diffusion and enhancing solution stability.

Although the tetrahedral mesh contains the largest number of computational elements, the resulting liquid fraction profile demonstrates the smoothest convergence trend among the investigated mesh configurations. Furthermore, comparison of the liquid fraction histories indicates that additional refinement beyond the selected tetrahedral mesh would be unlikely to produce significant changes in the predicted melting behaviour. Consequently, the numerical solution may be considered sufficiently independent of the computational grid.

## 3. Results and Discussion

### *3.1 Results*

#### *3.1.1 Liquid fraction evolution during PCM melting*

The melting behaviour of the phase change material (PCM) was investigated using the selected tetrahedral mesh obtained from the grid independence study. The evolution of the melting process was visualised using liquid fraction contours at different stages of the charging process. Three representative contour plots corresponding to the initial state, intermediate melting stage, and nearly complete melting condition were selected to illustrate the progression of the phase change process.

Figure 7 illustrates the temporal evolution of the liquid fraction within the PCM domain throughout the charging process. At the initial condition shown in Figure 7(a), the PCM remains completely solid with a liquid fraction of zero throughout the storage region. At this stage, thermal energy supplied by the heat transfer fluid has not yet generated sufficient heating to initiate the melting process.

As the charging process progresses, the PCM begins to melt near the heated inner tube wall, as shown in Figure 7(b). The increase in liquid fraction indicates that thermal energy has been transferred from the heat transfer fluid to the surrounding PCM through the copper tube wall. The molten region expands outward from the inner tube as the PCM absorbs sensible and latent heat, resulting in the gradual growth of the liquid phase within the storage domain.

Figure 7(c) presents the final stage of the charging process, where the liquid fraction reaches approximately 1, indicating that the PCM is almost completely melted. The liquid region occupies nearly the entire PCM domain, confirming that sufficient thermal energy has been supplied to complete the phase transition process. The progression observed in Figure 7 demonstrates the capability of the numerical model to capture the transient melting behaviour of the PCM and illustrates the overall charging mechanism of the latent heat thermal energy storage system.

The liquid fraction contours provide a qualitative representation of the phase change process and serve as the basis for evaluating the thermal performance of the storage system under different operating conditions. The selected tetrahedral mesh successfully captures the evolution of the melting front and provides a stable numerical representation of the PCM melting process throughout the simulation period.

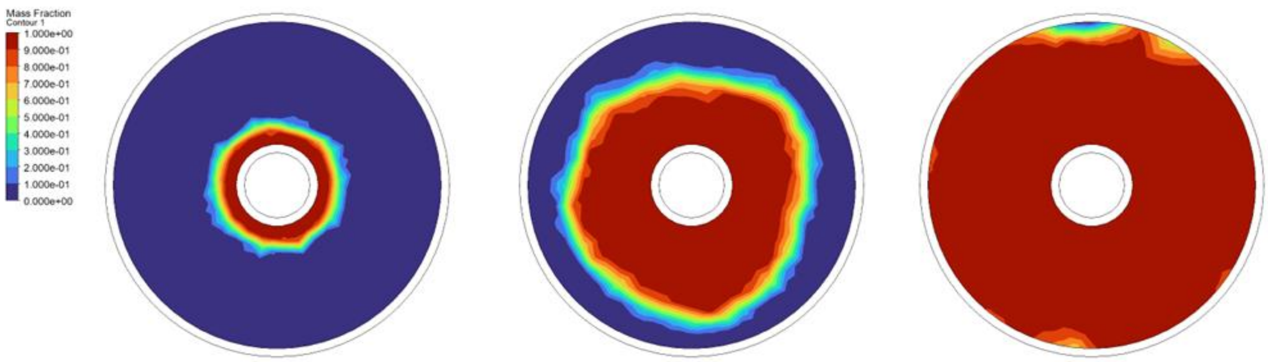


(a) (b) (c)

**Fig. 7.** Fluid fraction on different time step (s) (a) 0 s (b) 700 s (c) 1400 s

### *3.1.2 Effect of HTF velocity on liquid fraction evolution*

To evaluate the influence of heat transfer fluid (HTF) velocity on the melting performance of the latent heat thermal energy storage system, simulations were performed using inlet velocities of 20 m/s, 40 m/s, and 80 m/s while maintaining all other operating conditions constant. The variation of volume-averaged liquid fraction with flow time for the three velocity conditions is presented in Figure 8. All three velocity conditions exhibit a similar melting trend throughout the charging process. The liquid fraction increases continuously with time, indicating the gradual conversion of solid PCM into liquid PCM as thermal energy is transferred from the heat transfer fluid. Initially, the liquid fraction increases at a relatively uniform rate for all velocity conditions, indicating that the melting behaviour is nearly identical during the early stage of the charging process.

As the melting process progresses, slight differences begin to appear between the liquid fraction profiles. The simulation with an inlet velocity of 20 m/s exhibits a marginally higher liquid fraction during the intermediate stage of melting compared with the higher velocity cases. However, the differences remain relatively small throughout the simulation period. As the liquid fraction approaches unity, all three curves gradually converge and reach complete melting within a similar time range.

The results indicate that increasing the inlet velocity from 20 m/s to 80 m/s produces only a minor influence on the overall liquid fraction evolution. Although small variations can be observed during the intermediate melting stage, the general shape and progression of the liquid fraction curves remain largely unchanged. The similarity of the three profiles suggests that the PCM melting process is not significantly affected by the investigated velocity range under the present operating conditions.

Overall, the liquid fraction results demonstrate that the latent heat thermal energy storage system exhibits consistent melting behaviour across the investigated velocity conditions. The observed trends provide a basis for further discussion regarding the influence of heat transfer fluid velocity on the thermal performance of the storage system.

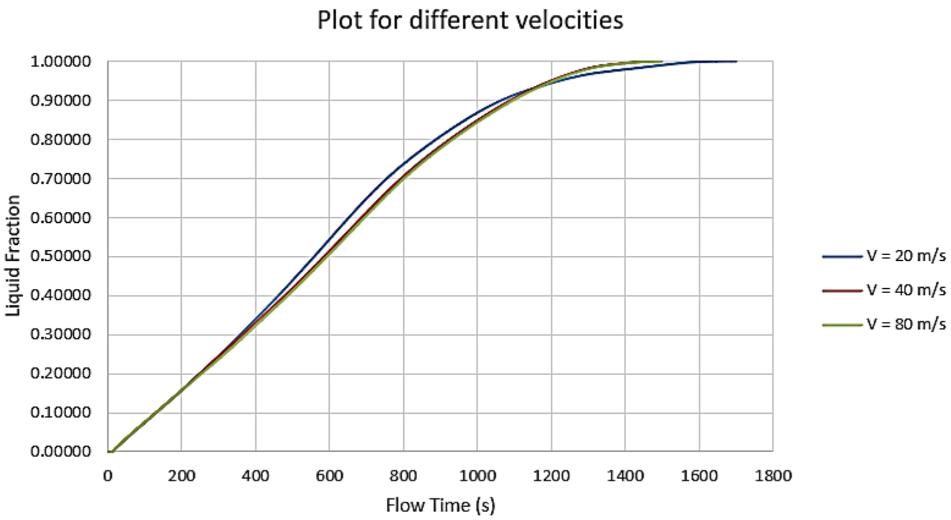


**Fig. 8.** Effect of HTF velocity on curve of liquid fraction

### *3.2 Discussion*

The liquid fraction contours and liquid fraction evolution curves presented in the previous section provide valuable insight into the melting behaviour of the PCM within the latent heat thermal energy storage system. The results demonstrate that the numerical model successfully captures the transient phase change process, beginning from a fully solid PCM state and progressing towards complete melting. The gradual increase in liquid fraction observed throughout the charging process confirms that thermal energy supplied by the heat transfer fluid is effectively transferred through the copper tube wall and subsequently absorbed by the PCM as sensible and latent heat.

The liquid fraction contours shown in Figure 7 reveal the progression of the melting front within the PCM domain. Initially, the PCM remains completely solid because the thermal energy supplied by the heat transfer fluid has not yet penetrated sufficiently into the storage region. As heating continues, melting begins in the vicinity of the inner tube wall where the temperature gradient is highest. This behaviour is expected because the tube wall acts as the primary heat transfer surface, resulting in the earliest phase transition occurring closest to the heat source. As additional thermal energy is transferred into the system, the molten region expands progressively outward from the tube wall until the liquid fraction approaches unity and the PCM becomes almost completely melted.

The observed melting behaviour is consistent with the physical characteristics of latent heat thermal energy storage systems reported in previous studies. During the early stages of charging, heat transfer within the PCM is primarily governed by thermal conduction because the material remains largely solid and fluid motion is absent. As melting progresses, liquid PCM begins to form around the heated tube, allowing buoyancy-driven flow to develop within the molten region. The resulting natural convection currents enhance thermal transport and contribute to the continued growth of the liquid phase. Similar melting patterns have been reported by Mahdi *et al.,* [19], who observed that natural convection becomes increasingly important as the volume of liquid PCM increases during the charging process.

The influence of heat transfer fluid velocity on the melting behaviour can be evaluated from the liquid fraction curves presented in Figure 8. Although three different inlet velocities were investigated, the resulting liquid fraction profiles exhibit only minor differences throughout the charging period. All velocity conditions produce a similar melting trend, characterised by a continuous increase in liquid fraction followed by complete melting within a relatively narrow time range. This observation suggests that the overall melting performance of the storage system is only weakly dependent on the investigated velocity range.

The limited influence of velocity can be explained by considering the dominant thermal resistance within the system. Increasing the HTF velocity generally enhances convective heat transfer inside the inner tube by reducing the thermal boundary layer thickness adjacent to the tube wall. However, once the thermal energy reaches the copper wall, it must still be conducted through the PCM and subsequently distributed throughout the storage region. Because paraffin-based PCMs possess relatively low thermal conductivity, the rate of heat transfer within the PCM domain becomes the controlling factor in the overall melting process. Consequently, further increases in HTF velocity provide only marginal improvements in melting performance because the dominant thermal resistance is located within the PCM rather than within the fluid flow region.

## 4. Conclusions

This study successfully investigated the melting behaviour of RT-50 phase change material (PCM) in a double-pipe latent heat thermal energy storage (LHTES) system using Computational Fluid Dynamics (CFD). A numerical model was developed in ANSYS Fluent by incorporating the laminar flow model, energy equation, and solidification–melting model based on the enthalpy–porosity formulation. The geometry and thermo-physical properties were adopted from a validated study in the literature, while a grid independence study was performed to ensure the reliability of the numerical results.

The first objective of this study, which was to simulate the melting process of RT-50 PCM during the charging process, was successfully achieved. The liquid fraction contours clearly illustrated the progression of the melting front from an initially solid state to a nearly fully melted condition. The second objective, which was to analyse the evolution of liquid fraction throughout the charging process, was also achieved. The liquid fraction profiles showed a continuous increase with flow time, indicating the gradual conversion of solid PCM into liquid PCM. The third objective of investigating the effect of HTF inlet velocity on PCM melting behaviour was accomplished by comparing liquid fraction evolution at inlet velocities of 20 m/s, 40 m/s, and 80 m/s. The results revealed that all velocity conditions produced similar melting trends and reached complete melting within a relatively narrow time range.

From an engineering perspective, the present findings suggest that increasing the HTF velocity beyond the baseline operating condition may not provide a proportionally significant improvement in thermal storage performance. Although higher velocities can increase the convective heat transfer coefficient within the tube, the resulting enhancement in PCM melting is relatively limited. Therefore, optimisation strategies focused solely on increasing fluid velocity may not be the most effective approach for improving charging performance. Instead, greater benefits may be achieved by enhancing heat transfer within the PCM domain through geometric modifications, increased heat transfer area, or the incorporation of thermal conductivity enhancement techniques.

Overall, the numerical results indicate that the melting behaviour of the PCM is governed primarily by the thermal characteristics of the storage medium and the heat transfer mechanisms occurring within the PCM region. The selected tetrahedral mesh successfully captures the evolution of the melting front and provides stable predictions of liquid fraction development throughout the charging process. Furthermore, the observed trends are consistent with previously published studies on PCM melting, providing confidence in the reliability of the numerical methodology and the validity of the simulation results.

## References

[1] Farid, Mohammed, Amar M. Khudhair, Siddique Ali K. Razack, and Said Al-Hallaj. "A review on phase change energy storage: materials and applications." *Thermal energy storage with phase change materials* (2021): 4-23. https://doi.org/10.1201/9780367567699-2

[2] Sharma, Atul, V. Veer Tyagi, Carl R. Chen, and Dharam Buddhi. "Review on thermal energy storage with phase change materials and applications." *Renewable and Sustainable energy reviews* 13, no. 2 (2009): 318-345. https://doi.org/10.1016/j.rser.2007.10.005

[3] Agyenim, Francis, Neil Hewitt, Philip Eames, and Mervyn Smyth. "A review of materials, heat transfer and phase change problem formulation for latent heat thermal energy storage systems (LHTESS)." *Renewable and Sustainable Energy Reviews* 14, no. 2 (2010): 615-628. https://doi.org/10.1016/j.rser.2009.10.015

[4] Kenisarin, Murat, and Khamid Mahkamov. "Solar energy storage using phase change materials." *Renewable and Sustainable Energy Reviews* 11, no. 9 (2007): 1913-1965. https://doi.org/10.1016/j.rser.2006.05.005

[5] Zalba, Belen, José Ma Marín, Luisa F. Cabeza, and Harald Mehling. "Review on thermal energy storage with phase change: materials, heat transfer analysis and applications." *Applied Thermal Engineering* 23, no. 3 (2003): 251-283. https://doi.org/10.1016/S1359-4311(02)00192-8

[6] Liu, Ming, Wasim Saman, and Frank Bruno. "Development of a novel refrigeration system for refrigerated trucks incorporating phase change material." *Applied Energy* 92 (2012): 336-342. https://doi.org/10.1016/j.apenergy.2011.10.015

[7] Sun, Zhigang, Tianfang Jiao, Zelin Ma, And Shanshan Liang. "Research on the enhancement of experimental methods for measuring thermal conductivity using the steady-state methods." *Physics and Engineering* 35, no. 4 (2025): 186-191. https://doi.org/10.26599/PHYS.2025.9320429

[8] Abhat, A. "Low temperature latent heat thermal energy storage: heat storage materials." *Solar Energy* 30, no. 4 (1983): 313-332. https://doi.org/10.1016/0038-092X(83)90186-X

[9] Ho Kon Tiat, Vanessa, and Elena Palomo del Barrio. "Recent patents on phase change materials and systems for latent heat thermal energy storage." *Recent Patents on Mechanical Engineering* 4, no. 1 (2011): 16-28. https://doi.org/10.2174/1874477X11104010016

[10] Trp, Anica. "An experimental and numerical investigation of heat transfer during technical grade paraffin melting and solidification in a shell-and-tube latent thermal energy storage unit." *Solar Energy* 79, no. 6 (2005): 648-660. https://doi.org/10.1016/j.solener.2005.03.006

[11] Hosseini, M. J., M. Rahimi, and R. Bahrampoury. "Experimental and computational evolution of a shell and tube heat exchanger as a PCM thermal storage system." *International Communications in Heat and Mass Transfer* 50 (2014): 128-136. https://doi.org/10.1016/j.icheatmasstransfer.2013.11.008

[12] Tay, N. H. S., F. Bruno, and M. Belusko. "Experimental validation of a CFD model for tubes in a phase change thermal energy storage system." *International Journal of Heat and Mass Transfer* 55, no. 4 (2012): 574-585. https://doi.org/10.1016/j.ijheatmasstransfer.2011.10.054

[13] Mahdi, Mustafa S., Hameed B. Mahood, Jasim M. Mahdi, Anees A. Khadom, and Alasdair N. Campbell. "Improved PCM melting in a thermal energy storage system of double-pipe helical-coil tube." *Energy Conversion and Management* 203 (2020): 112238. https://doi.org/10.1016/j.enconman.2019.112238

[14] Singh, Randeep, Sadegh Sadeghi, and Bahman Shabani. "Thermal conductivity enhancement of phase change materials for low-temperature thermal energy storage applications." *Energies* 12, no. 1 (2018): 75. https://doi.org/10.3390/en12010075

[15] Versteeg, Henk Kaarle. *An introduction to computational fluid dynamics the finite volume method, 2/E*. Pearson Education India, 2007.

[16] Voller, Vaughan R., and Chander Prakash. "A fixed grid numerical modelling methodology for convection-diffusion mushy region phase-change problems." *International Journal of Heat and Mass Transfer* 30, no. 8 (1987): 1709-1719. https://doi.org/10.1016/0017-9310(87)90317-6

[17] Arasu, A. Valan, and Arun S. Mujumdar. "Numerical study on melting of paraffin wax with Al2O3 in a square enclosure." *International Communications in Heat and Mass Transfer* 39, no. 1 (2012): 8-16. https://doi.org/10.1016/j.icheatmasstransfer.2011.09.013

[18] Al-Abidi, Abduljalil A., Sohif Mat, Kamaruzzaman Sopian, M. Y. Sulaiman, and Abdulrahman Th Mohammad. "Internal and external fin heat transfer enhancement technique for latent heat thermal energy storage in triplex tube heat exchangers." *Applied Thermal Engineering* 53, no. 1 (2013): 147-156. https://doi.org/10.1016/j.applthermaleng.2013.01.011

[19] Mahdi, Mustafa S., Hameed B. Mahood, Jasim M. Mahdi, Anees A. Khadom, and Alasdair N. Campbell. "Improved PCM melting in a thermal energy storage system of double-pipe helical-coil tube." *Energy Conversion and Management* 203 (2020): 112238. https://doi.org/10.1016/j.enconman.2019.112238

[20] Rakotondrandisa, Aina, Ionut Danaila, and Luminita Danaila. "Numerical modelling of a melting-solidification cycle of a phase-change material with complete or partial melting." *International Journal of Heat and Fluid Flow* 76 (2019): 57-71. https://doi.org/10.1016/j.ijheatfluidflow.2018.11.004